Empirical Natural Closure Relation for Short Fiber Suspension Models

E. Prulière [1], A. Ammar [1*], F. Chinesta [2]

[1] *Laboratoire de Rhéologie, INPG, UJF, CNRS (UMR 5520)*
1301 rue de la piscine, BP 53 Domaine universitaire
38041 Grenoble Cedex 9, France
pruliere@ujf-grenoble.fr
* *Amine.Ammar@ujf-grenoble.fr (corresponding author)*

[2] *LMSP UMR 8106 CNRS-ENSAM-ESEM*
151 Boulevard de l'Hôpital, F-75013 Paris, France
francisco.chinesta@paris.ensam.fr

ABSTRACT. This work focuses on the resolution of the Fokker-Planck equation that governs the evolution of the fibers orientation distribution. To reduce the computing time, that equation is solved along some flow trajectories in order to extract the significant information of the solution from the application of the Karhunen-Loève decomposition. Now, from this information one could solve the Fokker-Planck equation everywhere in the flow domain or simply adjust a closure relation that becomes optimal for such flow, solving the evolution of some orientation moments which require a less amount of computation. This paper focuses on this last strategy. For this purpose we start introducing the Karhunen-Loève decomposition that is applied later to automatically extract the main solution characteristics for adjusting empirically a natural closure relation.

KEYWORDS: Short fiber suspensions; Closure relations; Numerical modeling; Model reduction; Karhunen-Loève decomposition

1. Introduction

1.1. *Short Fiber Suspensions flow models*

Numerical modeling of non-Newtonian flows usually involves the coupling between equations of motion, which define an elliptic problem, and the fluid constitutive equation, which introduces an advection problem related to the fluid history. In short fiber suspensions (SFS) models, the extra-stress tensor depends on the fiber orientation whose evolution can be modeled from a transport problem. In all cases the flow kinematics and the fiber orientation are coupled: the kinematics of the flow governs the fiber orientation, and the presence and orientation of the fibers modify the flow kinematics. Thus, for example, in a contraction flow of a dilute suspension, large recirculating areas appear (Lipscomb et al. (1988)).

If one uses SFS flows in material forming processes, the final fiber orientation state depends on the process and exhibits flow-induced anisotropy. Thus, we need to compute the fiber orientation in order to predict the final mechanical properties of the composite parts, which depend strongly on the fiber orientation. Moreover, the numerical simulation of such flows becomes interesting if one wants to identify their rheological parameters using some rheometric devices and an appropriate inverse technique.

The mechanical model governing the SFS flow is given by the following equations: (Batchelor (1970), Hand (1962), Hinch and Leal (1975, 1976))

- The momentum balance equation, when the inertia and mass terms are neglected, results

  $$Div\underline{\underline{\sigma}} = \underline{0} \qquad (1)$$

  where $\underline{\underline{\sigma}}$ is the stress tensor.

- The mass balance equation for incompressible fluids

  $$Div\underline{v} = 0 \qquad (2)$$

  where $\underline{v}$ represents the velocity field.

- The constitutive equation for a dilute suspension of high aspect-ratio particles is given, with other simplifying assumptions (Tucker (1991)), by

$$\underline{\underline{\sigma}} = -p\underline{\underline{I}} + 2\eta\left\{\underline{\underline{D}} + N_p\left(\underline{\underline{\underline{\underline{a}}}} : \underline{\underline{D}}\right)\right\} \tag{3}$$

where p denotes the pressure, $\underline{\underline{I}}$ the unit tensor, η the viscosity which depends on the chosen model, $\underline{\underline{D}}$ the strain rate tensor, N_p a scalar parameter depending on both the fiber concentration and the fiber aspect ratio, " : " the tensorial product twice contracted (i.e. $\left(\underline{\underline{\underline{\underline{a}}}} : \underline{\underline{D}}\right)_{ij} = a_{ijkl} D_{kl}$) and $\underline{\underline{\underline{\underline{a}}}}$ the fourth order orientation tensor defined by:

$$\underline{\underline{\underline{\underline{a}}}} = \int \underline{\rho} \otimes \underline{\rho} \otimes \underline{\rho} \otimes \underline{\rho}\ \psi(\underline{\rho})\, d\underline{\rho} \tag{4}$$

where $\underline{\rho}$ is the unit vector aligned in the fiber axis direction, " $\otimes$ " denotes the tensorial product (i.e. $\left(\underline{\rho} \otimes \underline{\rho}\right)_{ij} = \rho_i \rho_j$), and $\psi(\underline{\rho})$ is the orientation distribution function satisfying the normality condition

$$\int \psi(\underline{\rho})\ d\underline{\rho} = 1 \tag{5}$$

If $\psi(\underline{\rho}) = \delta(\underline{\rho} - \underline{\hat{\rho}})$, with $\delta(\,)$ the Dirac's distribution, all the orientation probability is concentrated in the direction defined by $\underline{\hat{\rho}}$, and the corresponding orientation tensor results $\underline{\underline{\underline{\underline{\hat{a}}}}} = \underline{\hat{\rho}} \otimes \underline{\hat{\rho}} \otimes \underline{\hat{\rho}} \otimes \underline{\hat{\rho}}$.

We can also define the second order orientation tensor as:

$$\underline{\underline{a}} = \int \underline{\rho} \otimes \underline{\rho}\ \psi(\underline{\rho})\, d\underline{\rho} \tag{6}$$

It is easy to verify that if $\psi(\underline{\rho}) = \delta(\underline{\rho} - \underline{\hat{\rho}})$, the fourth order orientation tensor can be written as

$$\underline{\underline{\underline{\underline{a}}}} = \underline{\underline{a}} \otimes \underline{\underline{a}} \tag{7}$$

whose components are defined by $a_{ijkl} = a_{ij} a_{kl}$.

For general expressions of $\psi(\underline{\rho})$ the previous relation is not exact, and equation (7) becomes a closure approximation known as the quadratic closure relation: $a_{ijkl}^{quad} = a_{ij} a_{kl}$. However, other closure relations are usually applied (Advani and Tucker (1990), Dupret et al. (1998)), among them we can consider the linear closure relation:

$$a_{ijkl}^{lin} = -\frac{1}{(4+N_d)(2+N_d)}(\delta_{ij}\delta_{kl}+\delta_{ik}\delta_{jl}+\delta_{il}\delta_{jk}) + \frac{1}{(4+N_d)}(a_{ij}\delta_{kl}+a_{ik}\delta_{jl}+a_{il}\delta_{jk}+a_{kl}\delta_{ij}+a_{jl}\delta_{ik}+a_{jk}\delta_{il}) \quad (8)$$

where N_d refers to the space dimension, i.e.

$$N_d = \begin{cases} 2 & \text{in } 2D \\ 3 & \text{in } 3D \end{cases} \quad (9)$$

The hybrid closure relation

$$a_{ijkl}^{hyb} = f\ a_{ijkl}^{quad} + (1-f)\ a_{ijkl}^{lin} \quad (10)$$

where $f = \left(N_d\right)^{N_d} \det(\underline{\underline{a}})$; and finally, the natural closure relation (Dupret and Verleye (1999)) that in the 2D case takes the form

$$a_{ijkl}^{nat} = \frac{1}{6}\det(\underline{\underline{a}})(\delta_{ij}\delta_{kl}+\delta_{ik}\delta_{jl}+\delta_{il}\delta_{jk}) + \frac{1}{3}(a_{ij}a_{kl}+a_{ik}a_{jl}+a_{il}a_{jk}) \quad (11)$$

The 3D isotropic orientation state is defined by the uniform distribution function

$$\Psi\left(\underline{\rho}\right) = \frac{1}{4\pi} \quad (12)$$

and then, the second order orientation tensor related to that isotropic orientation state is

$$\underline{\underline{a}} = \frac{\underline{\underline{I}}}{3} \quad (13)$$

It is easy to verify that for isotropic orientation distributions (2D or 3D) the linear closure becomes exact.

- If we consider spheroidal fibers immersed in a dilute suspension, we can describe the orientation evolution by means of the Jeffery equation (Jeffery (1922))

$$\frac{d\underline{\rho}}{dt} = \underline{\underline{\Omega}}\ \underline{\rho} + k\left(\ \underline{\underline{D}}\ \underline{\rho} - \left(\underline{\underline{D}} : \left(\ \underline{\rho}\otimes\underline{\rho}\ \right)\right)\ \ \underline{\rho}\ \right) \quad (14)$$

where $\underline{\underline{\Omega}}$ is the vorticity tensor, and k is a constant that depends on the fiber aspect ratio r (fiber length to fiber diameter ratio):

$$k = \left(r^2 - 1\right) \Big/ \left(r^2 + 1\right) \tag{15}$$

On the other hand the evolution of the fiber orientation distribution ψ is governed by the Fokker-Planck equation,

$$\frac{d\psi(\underline{\rho})}{dt} + \frac{\partial}{\partial \underline{\rho}} \left\{ \psi(\underline{\rho}) \frac{d\underline{\rho}}{dt} \right\} = 0 \tag{16}$$

where the material derivative is given by:

$$\frac{d\psi}{dt} = \frac{\partial \psi}{\partial t} + \underline{v}\ Grad\psi \tag{17}$$

Now, taking into account equations (6), (14) and (16), the equation that governs the evolution of the second order orientation tensor can be deduced

$$\frac{d\underline{\underline{a}}}{dt} = \underline{\underline{\Omega}}\ \underline{\underline{a}} - \underline{\underline{a}}\ \underline{\underline{\Omega}} + k\left(\underline{\underline{D}}\ \underline{\underline{a}} + \underline{\underline{a}}\ \underline{\underline{D}} - 2\left(\underline{\underline{a}} : \underline{\underline{D}}\right)\right) \tag{18}$$

A similar equation can be derived for the evolution of the fourth order orientation tensor, which in this case involves the sixth-order orientation tensor.

To take account of fiber interaction effects in semi-concentrated suspensions Folgar and Tucker (1984) proposed the introduction of a diffusion term in the Fokker-Planck equation, i.e.

$$\frac{d\psi(\underline{\rho})}{dt} + \frac{\partial}{\partial \underline{\rho}} \left\{ \psi(\underline{\rho}) \frac{d\underline{\rho}}{dt} \right\} = \frac{\partial}{\partial \underline{\rho}} \left\{ D_r \frac{\partial \psi(\underline{\rho})}{\partial \underline{\rho}} \right\} \tag{19}$$

Fiber interaction being taken into account, the equation governing the evolution of $\underline{\underline{a}}$ then yields:

$$\frac{d\underline{\underline{a}}}{dt} = \underline{\underline{\Omega}}\ \underline{\underline{a}} - \underline{\underline{a}}\ \underline{\underline{\Omega}} + k\left(\underline{\underline{D}}\ \underline{\underline{a}} + \underline{\underline{a}}\ \underline{\underline{D}} - 2\left(\underline{\underline{a}} : \underline{\underline{D}}\right)\right) - 4D_r\left(\underline{\underline{a}} - \frac{\underline{\underline{I}}}{N_d}\right) \tag{20}$$

The Fokker-Planck formalism circumvents the necessity of using closure relations, but it induces some difficulties related to its multidimensional character (the distribution function is defined in the physical and the configuration spaces) and moreover advection terms are defined in both spaces. By these reasons the

number of works devoted to the treatment of the FP equation is relatively reduced (Lozinski and Chauvière (2003); Chauvière and Lozinski (2004)). In these techniques, usually, to account for the multidimensional character of the FP equation, a time-splitting is often considered to decouple the advection problem in physical space and the advection-diffusion problem in the conformation space. The first problem can be solved by a numerical method appropriate for hyperbolic partial differential equations (discontinuous Galerkin, SUPG, …). Then, the advection-diffusion problem defined in the conformation space can be treated using different implicit techniques (SUPG, wavelets-Galerkin, spectral techniques, …) preserving stability, accounting for distribution relatively localized as well as periodic boundary conditions in the conformation space.

In general we can solve the FP equation from its associated Ito stochastic differential equation for a large set of realizations. The CONNFFESSIT method (Ottinger and Laso (1992)) was the first implementation of the stochastic approach. The Brownian Configuration Fields (Hulsen et al. (1997)) can be considered as an improvement of the CONNFFESSIT method. However, the control of the statistical noise is a major issue in stochastic micro-macro simulations, problem that does not arise in the deterministic Fokker-Planck approach.

This work focuses on the resolution of the Fokker-Planck equation that governs the evolution of the fibers orientation distribution. To reduce the computing time, that equation is solved along some flow trajectories in order to extract the significant information of the solution from the application of the Karhunen-Loève decomposition. Now, from this information one could solve the Fokker-Planck equation everywhere in the flow domain or simply adjust a closure relation that becomes optimal for such flow, solving the evolution of some orientation moments which require a less amount of computation. Some antecedents exist concerning closure relation fitting; see for example Parsheh et al. (2006) or Gillet-Chaulet et al. (2006). The present paper focuses on the definition of an empirical natural closure approximation for each particular flow. For this purpose we start introducing the Karhunen-Loève decomposition (Ryckelynck et al. (2006)) that is applied later to automatically extract the main solution characteristics for adjusting empirically a natural closure relation.

1.2. ***The Karhunen-Loève decomposition***

We assume that the evolution of a certain field $u(\underline{x},t)$ is known. In practical applications, this field is expressed in a discrete form, that is, it is known at the nodes of a spatial mesh and for some times $u(\underline{x}_i,t^p)\equiv u_i^p$. We can also write introducing a spatial interpolation $u^p(\underline{x}_i)\equiv u(\underline{x}_i,t=p\Delta t)$, $\forall p\in[1,\cdots,P]\ \ \forall i\in[1,\cdots,N]$. The main idea of the Karhunen-Loève (*KL*) decomposition is how to obtain the most typical or characteristic structure $\phi(\underline{x})$ among these $u^p(\underline{x}),\forall p$. This is equivalent to obtaining a function $\phi(\underline{x})$ that maximizes α.

$$\alpha=\frac{\sum_{p=1}^{p=P}\left[\sum_{i=1}^{i=N}\phi(\underline{x}_i)\ u^p(\underline{x}_i)\right]^2}{\sum_{i=1}^{i=N}\left(\phi(\underline{x}_i)\right)^2} \tag{21}$$

The maximization leads to:

$$\begin{aligned}\sum_{p=1}^{p=P}\left[\left[\sum_{i=1}^{i=N}\tilde{\phi}(\underline{x}_i)\ u^p(\underline{x}_i)\right]\left[\sum_{j=1}^{j=N}\phi(\underline{x}_j)\ u^p(\underline{x}_j)\right]\right]=\\ =\alpha\sum_{i=1}^{i=N}\tilde{\phi}(\underline{x}_i)\ \phi(\underline{x}_i)\ ;\ \ \forall\tilde{\phi}\end{aligned} \tag{22}$$

which can be rewritten in the form

$$\begin{aligned}\sum_{i=1}^{i=N}\left[\sum_{j=1}^{j=N}\left\{\sum_{p=1}^{p=P}u^p(\underline{x}_i)\ u^p(\underline{x}_j)\ \phi(\underline{x}_j)\right\}\tilde{\phi}(\underline{x}_i)\right]=\\ =\alpha\sum_{i=1}^{i=N}\tilde{\phi}(\underline{x}_i)\ \phi(\underline{x}_i)\ ;\quad\forall\tilde{\phi}\end{aligned} \tag{23}$$

Defining the vectors $\underline{a}$ such that its i-component is $a(\underline{x}_i)$, Eq. (23) takes the following matrix form

$$\underline{\tilde{\phi}}^T\ \underline{\underline{k}}\ \underline{\phi}=\alpha\ \underline{\tilde{\phi}}^T\ \underline{\phi}\ ;\quad\forall\underline{\tilde{\phi}}\quad\Rightarrow\quad\underline{\underline{k}}\ \underline{\phi}=\alpha\underline{\phi} \tag{24}$$

where the two points correlation matrix is given by

$$k_{ij}=\sum_{p=1}^{p=P}u^p(\underline{x}_i)\ u^p(\underline{x}_j)\ \Leftrightarrow\underline{\underline{k}}=\sum_{p=1}^{p=P}\underline{u}^p\left(\underline{u}^p\right)^T \tag{25}$$

which is symmetric and positive definite. If we define the matrix $\underline{\underline{Q}}$ containing the discrete field history:

$$\underline{\underline{Q}} = \begin{pmatrix} u_1^1 & u_1^2 & \cdots & u_1^P \\ u_2^1 & u_2^2 & \cdots & u_2^P \\ \vdots & \vdots & \ddots & \vdots \\ u_N^1 & u_N^2 & \cdots & u_N^P \end{pmatrix} \tag{26}$$

is easy to verify that the matrix $\underline{\underline{k}}$ in Eq. (25) results:

$$\underline{\underline{k}} = \underline{\underline{Q}}\ \underline{\underline{Q}}^T \tag{27}$$

1.3 ***"A posteriori" reduced modeling***

If some direct simulations are carried out, we can determine $u\left(\underline{x}_i, t^p\right) \equiv u_i^p, \forall i \in [1,\cdots,N], \forall p \in [1,\cdots,P]$, and from these the n eigenvectors related to the n-highest eigenvalues $\underline{\phi}_k = \phi_k\left(\underline{x}_i\right), \forall i \in [1,\cdots,N], \forall k \in [1,\cdots,n]$ that are expected to contain the most information about the problem solution. For this purpose we solve the eigenvalue problem defined by Eq. (24) retaining all the eigenavules belonging to the interval defined by the highest eigenvalue and that value divided by a large enough value (10^8 in our simulations). In practice n is much lower than N. Thus, we can try to use these n eigenfunctions for approximating the solution of a problem slightly different to the one that has served to define $u\left(\underline{x}_i, t^p\right) \equiv u_i^p$. For this purpose we need to define the matrix $\underline{\underline{B}}$

$$\underline{\underline{B}} = \begin{pmatrix} \phi_1\left(\underline{x}_1\right) & \phi_2\left(\underline{x}_1\right) & \cdots & \phi_n\left(\underline{x}_1\right) \\ \phi_1\left(\underline{x}_2\right) & \phi_2\left(\underline{x}_2\right) & \cdots & \phi_n\left(\underline{x}_2\right) \\ \vdots & \vdots & \ddots & \vdots \\ \phi_1\left(\underline{x}_N\right) & \phi_2\left(\underline{x}_N\right) & \cdots & \phi_n\left(\underline{x}_N\right) \end{pmatrix} \tag{28}$$

Now, if we consider the linear system of equations resulting from the discretization of a partial differential equation (PDE) in the form

$$\underline{\underline{K}}\ \underline{U}^{(m)} = \underline{F}^{(m-1)} \tag{29}$$

where the superscript refers to the time step, then, assuming that the unknown vector contains the nodal degrees of freedom, it can be expressed as:

$$\underline{U}^{(m)} = \sum_{i=1}^{i=n} \zeta_i^{(m)} \underline{\phi}_i = \underline{\underline{B}}\ \underline{\zeta}^{(m)} \tag{30}$$

Eq. (29) results

$$\underline{\underline{K}}\ \underline{U}^{(m)} = \underline{F}^{(m-1)} \Rightarrow \underline{\underline{K}}\ \underline{\underline{B}}\ \underline{\zeta}^{(m)} = \underline{F}^{(m-1)} \tag{31}$$

and by multiplying both terms by $\underline{\underline{B}}^T$ it results

$$\underline{\underline{B}}^T\ \underline{\underline{K}}\ \underline{\underline{B}}\ \underline{\zeta}^{(m)} = \underline{\underline{B}}^T\ \underline{F}^{(m-1)} \tag{32}$$

which proves that the final system of equations is of low order, i.e. the dimension of $\underline{\underline{B}}^T\ \underline{\underline{K}}\ \underline{\underline{B}}$ is $n \times n$, with $n << N$, and the dimensions of both $\underline{\zeta}^{(m)}$ and $\underline{\underline{B}}^T\ \underline{F}^{(m-1)}$ are $n \times 1$.

Remark 1. Equation (32) can be also derived introducing the approximation (30) into the PDE Galerkin form.

2. Simulating complex flows

We consider the use of a decoupled strategy which solves the flow kinematics (from the orientation state known at the previous iteration or time step), and then the orientation state can be updated using the velocity field just computed. The flow kinematics can be solved accurately by using standard discretization techniques as for example the finite element method. This paper focuses on the resolution of the orientation problem which involves some specific difficulties.

2.1 *Extracting the solution structure*

One possibility for reducing the computing time associated with the resolution of the Fokker-Planck equation (18) consists of decoupling the resolution of the purely advection problem in the physical space and the advection-diffusion defined in the conformation space. Now, the first problem can be accurately integrated using the method of characteristics along some nodal trajectories, being the one defined in the conformation space discretized using some stabilized finite element strategy for accounting its advection character. The model reduction described later will operate only on the conformation space discretization.

We briefly summarize this strategy in the 2D case, the 3D case being a direct extension. In that case the Fokker-Planck equation can be written using polar coordinates as:

$$\frac{d\psi(\underline{x},\varphi,t)}{dt}+\frac{\partial}{\partial\varphi}\left\{\psi(\underline{x},\varphi,t)\left.\frac{d\varphi}{dt}\right|_{\underline{x},\varphi,t}\right\}=\frac{\partial}{\partial\varphi}\left\{D_r\frac{\partial\psi(\underline{x},\varphi,t)}{\partial\varphi}\right\} \tag{33}$$

where $\left.\frac{d\varphi}{dt}\right|_{\underline{x},\varphi,t}$ is computed from the Jeffery equation (13):

$$\begin{pmatrix}-\sin\varphi\\ \cos\varphi\end{pmatrix}\frac{d\varphi}{dt}=\begin{pmatrix}0 & \Omega_{12}\\ -\Omega_{12} & 0\end{pmatrix}\begin{pmatrix}\cos\varphi\\ \sin\varphi\end{pmatrix}+k\begin{pmatrix}D_{11} & D_{12}\\ D_{12} & -D_{11}\end{pmatrix}\begin{pmatrix}\cos\varphi\\ \sin\varphi\end{pmatrix}-$$
$$-k\left(\begin{pmatrix}\cos\varphi & \sin\varphi\end{pmatrix}\begin{pmatrix}D_{11} & D_{12}\\ D_{12} & -D_{11}\end{pmatrix}\begin{pmatrix}\cos\varphi\\ \sin\varphi\end{pmatrix}\right)\begin{pmatrix}\cos\varphi\\ \sin\varphi\end{pmatrix} \tag{34}$$

By multiplying the second equation by $\cos\varphi$, the first one by $\sin\varphi$ and subtracting the first one from the second one, it results:

$$\frac{d\varphi}{dt}=\begin{pmatrix}-\sin\varphi & \cos\varphi\end{pmatrix}\begin{pmatrix}0 & \Omega_{12}\\ -\Omega_{12} & 0\end{pmatrix}\begin{pmatrix}\cos\varphi\\ \sin\varphi\end{pmatrix}+$$
$$+k\begin{pmatrix}-\sin\varphi & \cos\varphi\end{pmatrix}\begin{pmatrix}D_{11} & D_{12}\\ D_{12} & -D_{11}\end{pmatrix}\begin{pmatrix}\cos\varphi\\ \sin\varphi\end{pmatrix} \tag{35}$$

where the components of both the vorticity and the strain rate tensor could depend on the physical coordinates $\underline{x}$ and time t.

Applying a stabilized finite element discretization of Eq. (33) in the conformation space (φ) it results (taking into account the solution periodicity in the angular coordinate):

$$\int_0^{2\pi}\psi^*\frac{d\psi}{dt}d\varphi+\int_0^{2\pi}\overline{\psi}^*\frac{d\varphi}{dt}\frac{\partial\psi}{\partial\varphi}d\varphi+\int_0^{2\pi}\psi^*\psi\frac{\partial}{\partial\varphi}\left\{\frac{d\varphi}{dt}\right\}d\varphi=$$
$$=-\int_0^{2\pi}D_r\frac{\partial\psi^*}{\partial\varphi}\frac{\partial\psi}{\partial\varphi}d\varphi \tag{36}$$

The weighting function ψ^* is approximated as ψ whereas $\overline{\psi}^*$ is approximated in a different way in order to account for the advection character of the differential operation. Different alternatives exist, out of the scope of the present work. In our simulations a SUPG (streamline upwind Petrov Galerkin) stabilization has been used. Finally, after introducing the different finite element interpolations and perform the numerical integration the following linear system is obtained:

$$\underline{\underline{K}}_1 \dot{\underline{\psi}} = \underline{\underline{K}}_2 \underline{\psi} + \underline{F} \Rightarrow \dot{\underline{\psi}} = \underline{\underline{K}}_1^{-1} \underline{\underline{K}}_2 \underline{\psi} + \underline{\underline{K}}_1^{-1} \underline{F} \tag{37}$$

In this equation vector $\underline{F}$ accounts for the normality condition of the orientation distribution that is enforced using a Lagrange multiplier technique.

Now, for integrating in the physical domain we use the method of characteristics by its simplicity and high accuracy. For this purpose, we assume that we are looking for the solution along the streamline related to point $\underline{X}$ where at the initial time *t=0* the orientation distribution is known.

Now, the orientation distribution updating is given by:

$$\begin{cases} \underline{x}(t_{n+1};\underline{X},t=0) = \underline{x}(t_n;\underline{X},t=0) + \underline{v}(\underline{x}(t_n;\underline{X},t=0),t_n)\,\Delta t \\ \underline{\psi}(\underline{x}(t_{n+1};\underline{X},t=0),t_{n+1}) = \underline{\psi}(\underline{x}(t_n;\underline{X},t=0),t_n) + \\ \qquad + \underline{\underline{K}}_1^{-1}\left[\underline{\underline{K}}_2 \underline{\psi}(\underline{x}(t_n;\underline{X},t=0),t_n) + \underline{F}\right]\Delta t \end{cases} \tag{38}$$

where $\underline{x}(t_{n+1};\underline{X},t=0)$ denotes the position that at time t_{n+1} occupies a fluid volume located at point $\underline{X}$ at time *t=0.*

Using this simple uncoupled strategy one can compute the evolution of the fiber orientation distribution along some nodal trajectories identified by the parameter *l*. Those distributions could be stored at some time steps (snapshots) leading to the following eigenvalue problems:

$$\underline{\underline{Q}}_{(l)}\underline{\underline{Q}}_{(l)}\,\underline{\phi}^{(l)} = \alpha\underline{\phi}^{(l)}; \quad l \in [1,\cdots,L] \tag{39}$$

with

$$\underline{\underline{Q}}_{(l)} = \begin{pmatrix} {}_{(l)}\psi_1^1 & {}_{(l)}\psi_1^2 & \cdots & {}_{(l)}\psi_1^{P_l} \\ {}_{(l)}\psi_2^1 & {}_{(l)}\psi_2^2 & \cdots & {}_{(l)}\psi_2^{P_l} \\ \vdots & \vdots & \ddots & \vdots \\ {}_{(l)}\psi_{N_c}^1 & {}_{(l)}\psi_{N_c}^2 & \cdots & {}_{(l)}\psi_{N_c}^{P_l} \end{pmatrix} \tag{40}$$

where (l) denotes the nodal trajectory, P_l the number of the selected distributions along each trajectory (snapshots), and L is the total number of nodal trajectories where the Fokker-Planck equation has been integrated, of course, $L << N$, with N the total number of nodes used to discretize the physical domain where the flow is defined and N_c the number of nodes used in the conformation space discretization (φ). Now, from the solution of Eq. (39) we can compute the most significant eignfunctions allowing to write:

$${}_{(l)}\underline{\psi}(t) \approx \sum_{i=1}^{i=n_l} \zeta_i^{(l)}(t)\underline{\phi}_i^{(l)} = \underline{\underline{B}}^{(l)} \ \underline{\zeta}^{(l)}(t) \tag{41}$$

Vector $\underline{\psi}$ has N_c components that are in fact the values of the distribution function at the nodes used to discretize the conformation domain (the unit circle or the unit surface in the 2D or 3D case respectively).

Now we will define a global reduced approximation basis $\underline{\underline{B}}$ from the different reduced approximation bases $\underline{\underline{B}}^{(l)}$. For this purpose, we proceed as follows:

- $\underline{\underline{B}} = \underline{\underline{B}}^{(1)}$, $n = n_1$ and l=1
- While $l \le L$
    - $l \leftarrow l+1$
    - $i = 0$
    - While $i \le n_l$
        - $i \leftarrow i+1$
        - If $\left\| \underline{\phi}_i^{(l)} - \sum_{j=1}^{n} \left[\left(\underline{\phi}_i^{(l)} \right)^T \underline{\phi}_j \right] \underline{\phi}_j \right\| > TOL$
            - $\underline{\underline{B}} = \left[\underline{\underline{B}} \ \underline{\phi}_i^{(l)} \right]$
            - $n \leftarrow n+1$

that is, we update the reduced approximation basis introducing only vectors that are not too close to the existing ones (for a given tolerance *TOL*).

The final reduced approximation basis consists of the *n* vectors contained in matrix $\underline{\underline{B}}$, and it could be expected that that basis represents accurately all the orientation distributions in the whole flow domain.

In order to accelerate the computation it could be interesting to solve the equation governing the evolution of the second order orientation equation instead of the resolution of the Fokker-Planck equation, along all the nodal trajectories, but as previously argued this approach involves the introduction of an appropriate closure relation allowing the expression of the fourth order orientation tensor from the expression of the second order one.

Remark 2. It is also possible to derive an evolution equation for the fourth order orientation tensor that involves the sixth order one, and also requires the definition of an appropriate closure relation. Despite that, this strategy could be more appealing because the constitutive equation directly uses the fourth order orientation tensor, and the procedure described in this work could be applied for deriving this closure relation, from now on we only consider the evolution problem related to the second order tensor and the associated closure problem.

Now, we denote by $\underline{\phi}_j ; j \in [1, \cdots, n]$ the n approximation vectors contained in matrix $\underline{\underline{B}}$, that are expected to describe accurately the evolution of the orientation distribution solution along any flow streamline, i.e.

$$\underline{\psi}(\underline{x}(t;\underline{x}_0, t=0)) \approx \sum_{i=1}^{i=n} \zeta_i(t)\underline{\phi}_i = \underline{\underline{B}}\ \underline{\zeta}(t) \qquad (42)$$

where $\underline{x}(t;\underline{x}_0, t=0)$ denotes the position at time *t* of a fluid particle located at $\underline{x}_0$ at time $t=0$.

Taking into account the expressions of the second and fourth order orientation tensors, given by Eqs. (6) and (4) respectively, it results:

$$ {}_{(2)}\underline{a}(\underline{x}(t;\underline{x}_0,t=0)) \approx \sum_{i=1}^{i=n} \zeta_i(t)\, {}_{(2)}\underline{a}_i = {}_{(2)}\underline{\underline{A}}\ \underline{\zeta}(t) \tag{43} $$

and

$$ {}_{(4)}\underline{a}(\underline{x}(t;\underline{x}_0,t=0)) \approx \sum_{i=1}^{i=n} \zeta_i(t)\, {}_{(4)}\underline{a}_i = {}_{(4)}\underline{\underline{A}}\ \underline{\zeta}(t) \tag{44} $$

where ${}_{(2)}\underline{a}$ and ${}_{(4)}\underline{a}$ denote the vector form of the second and fourth order orientation tensors respectively, being ${}_{(2)}\underline{a}_i$ and ${}_{(4)}\underline{a}_i$ the vector forms of the tensors defined by the integrals:

$$ \underline{\underline{\underline{a}}}_i = \int_0^{2\pi} \underline{\rho} \otimes \underline{\rho} \otimes \underline{\rho} \otimes \underline{\rho}\ \phi_i(\varphi)\, d\varphi \qquad \text{with} \qquad \underline{\rho} = \begin{pmatrix} \cos\varphi \\ \sin\varphi \end{pmatrix} \tag{45} $$

and

$$ \underline{\underline{a}}_i = \int_0^{2\pi} \underline{\rho} \otimes \underline{\rho}\ \phi_i(\varphi)\, d\varphi \tag{46} $$

We would mention that the value of $\phi_i(\varphi)$ at point φ can be determined by standard interpolation from the nodal values of ϕ_i contained in the vector $\underline{\phi}_i$. Finally, matrix ${}_{(2)}\underline{\underline{A}}$ and ${}_{(4)}\underline{\underline{A}}$ are built from vectors ${}_{(2)}\underline{a}_i$ and ${}_{(4)}\underline{a}_i$ which defines their different columns.

2.2 *Natural closure relation*

Any closure approximation of the fourth order orientation tensor can be written using the Caley-Hamilton theorem as well as partial normalization and symmetry (see Dupret and Verleye, 1999), in the general form:

$$ \begin{cases} {}_{(4)}\underline{a} = \sum_{i=1}^{i=6} {}_{(4)}\underline{w}_{\mathrm{i}}\ \beta_i & \text{in} \quad 3\mathrm{D} \\ {}_{(4)}\underline{a} = \sum_{i=1}^{i=3} {}_{(4)}\underline{w}_{\mathrm{i}}\ \beta_i & \text{in} \quad 2\mathrm{D} \end{cases} \tag{47} $$

where

$$\begin{cases} {}_{(4)}\underline{\underline{w}}_1 = S(\underline{\underline{I}} \otimes \underline{\underline{I}}) \\ {}_{(4)}\underline{\underline{w}}_2 = S(\underline{\underline{I}} \otimes \underline{\underline{a}}) \\ {}_{(4)}\underline{\underline{w}}_3 = S(\underline{\underline{a}} \otimes \underline{\underline{a}}) \\ {}_{(4)}\underline{\underline{w}}_4 = S(\underline{\underline{I}} \otimes \underline{\underline{a}}^2) \\ {}_{(4)}\underline{\underline{w}}_5 = S(\underline{\underline{a}} \otimes \underline{\underline{a}}^2) \\ {}_{(4)}\underline{\underline{w}}_6 = S(\underline{\underline{a}}^2 \otimes \underline{\underline{a}}^2) \end{cases} \tag{48}$$

and where $S(\ )$ refers to the symmetric component.

All the coefficients β_i are not independent due to the normalization conditions. Thus, we have in 3D

$$\begin{pmatrix} 10 & 1 & 0 \\ 0 & 7 & 2 \\ 0 & 0 & 4 \end{pmatrix} \begin{pmatrix} \beta_1 \\ \beta_2 \\ \beta_3 \end{pmatrix} = - \begin{pmatrix} 1-2D & 4P & 4P \\ 0 & 1-6D & 4(P-D) \\ 7 & 5 & 2(3-4D) \end{pmatrix} \begin{pmatrix} \beta_4 \\ \beta_5 \\ \beta_6 \end{pmatrix} + \begin{pmatrix} 0 \\ 6 \\ 0 \end{pmatrix} \tag{49}$$

and in 2D

$$\begin{pmatrix} 8 & 1 \\ 0 & 1 \end{pmatrix} \begin{pmatrix} \beta_1 \\ \beta_2 \end{pmatrix} = - \begin{pmatrix} -4P \\ 1 \end{pmatrix} \beta_3 + \begin{pmatrix} 0 \\ 1 \end{pmatrix} \tag{50}$$

where $P = \det(\underline{\underline{a}})$ and $D = \frac{1}{2}\left(1 - Tr\left(\underline{\underline{a}}^2\right)\right)$ (with *Tr* () the tensor trace).

From now on, and for the sake of generality, we consider the 3D case. Thus, Eq. (49) can be written in the matrix form:

$$\underline{\underline{f}}\ \underline{\beta}_u = \underline{\underline{g}}\ \underline{\beta}_d + \underline{h} \tag{51}$$

Eq. (47) results:

$${}_{(4)}\underline{\underline{a}} = \sum_{i=1}^{i=6} {}_{(4)}\underline{\underline{w}}_i\ \beta_i = \underline{\underline{W}}\,\underline{\beta} = \underline{\underline{W}} \begin{pmatrix} \underline{\beta}_u \\ \underline{\beta}_d \end{pmatrix} = \underline{\underline{W}} \begin{pmatrix} \underline{\underline{f}}^{-1}\underline{\underline{g}} \\ \underline{\underline{I}} \end{pmatrix} \underline{\beta}_d + \underline{\underline{W}} \begin{pmatrix} \underline{\underline{f}}^{-1}\underline{h} \\ \underline{0} \end{pmatrix} = \tag{52}$$
$$= \underline{\underline{\widehat{W}}}\,\underline{\beta}_d + \underline{\breve{W}}$$

Now, considering Eq. (52) for the *n* couples of tensors $\left[\underline{\underline{a}}_i\ ,\ \underline{\underline{a}}_i\right]$ extracted from the most significant distribution functions (as explained in the previous section), one could be interested in determining the optimal value of $\underline{\beta}_d$, that is close to the procedure used by Dupret and Verleye to derive the natural

closure relation, but they considered only the distribution related to an initial isotropic distribution of infinite slender fibers, without diffusion effects and in a simple shear flow.

2.3 *Local natural closure relation*

For computing the unknown beta coefficients we proceed by using a moving least square technique. For this purpose we define the approximation error

$$J({}_{(2)}\underline{a},\underline{\beta}_d)=\sum_{i=1}^{i=n}\delta_\varepsilon\left(\left\|{}_{(2)}\underline{a}-{}_{(2)}\underline{a}_i\right\|\right)\,\gamma_i\,\left[{}_{(4)}\underline{a}_i-\underline{\underline{\widehat{W}}}_i\underline{\beta}_d-\underline{\breve{W}}_i\right]^2 \tag{53}$$

where the weighting coefficient γ_i scales with λ_i related to the eigenfunction $\underline{\phi}_i$ that was used for computing tensors $\underline{\underline{\underline{a}}}_i$ and $\underline{\underline{a}}_i$. The window function $\delta_\varepsilon(d)$ is introduced for increasing the weight of closer couples $\left[\underline{\underline{\underline{a}}}_i\,,\,\underline{\underline{a}}_i\right]$ in the error expression. In our simulations we have considered the following window function:

$$\delta_\varepsilon(d)=\frac{\delta\left(\frac{d}{\varepsilon}\right)}{\varepsilon}\quad\text{with}\quad\delta\left(\frac{d}{\varepsilon}\right)=\frac{e^{-\left(\frac{d}{\varepsilon}\right)^2}}{\sqrt{\pi}} \tag{54}$$

Now, the optimality condition implies

$$\frac{\partial J}{\partial\underline{\beta}_d}=\underline{0}=2\sum_{i=1}^{i=n}\delta_\varepsilon\left(\left\|{}_{(2)}\underline{a}-{}_{(2)}\underline{a}_i\right\|\right)\,\gamma_i\,\underline{\underline{\widehat{W}}}_{\mathrm{i}}^{\mathrm{T}}\,\left[{}_{(4)}\underline{a}_i-\underline{\underline{\widehat{W}}}_i\underline{\beta}_d-\underline{\breve{W}}_i\right] \tag{55}$$

that is:

$$\begin{aligned}\left[\sum_{i=1}^{i=n}\delta_\varepsilon\left(\left\|{}_{(2)}\underline{a}-{}_{(2)}\underline{a}_i\right\|\right)\,\gamma_i\,\underline{\underline{\widehat{W}}}_{\mathrm{i}}^{\mathrm{T}}\,\underline{\underline{\widehat{W}}}_i\right]\underline{\beta}_d=\\ =\sum_{i=1}^{i=n}\delta_\varepsilon\left(\left\|{}_{(2)}\underline{a}-{}_{(2)}\underline{a}_i\right\|\right)\,\gamma_i\,\underline{\underline{\widehat{W}}}_{\mathrm{i}}^{\mathrm{T}}\,\left[{}_{(4)}\underline{a}_i-\underline{\breve{W}}_i\right]\end{aligned} \tag{56}$$

or

$$\begin{aligned}\underline{\beta}_d=\left[\sum_{i=1}^{i=n}\delta_\varepsilon\left(\left\|{}_{(2)}\underline{a}-{}_{(2)}\underline{a}_i\right\|\right)\,\gamma_i\,\underline{\underline{\widehat{W}}}_{\mathrm{i}}^{\mathrm{T}}\,\underline{\underline{\widehat{W}}}_i\right]^{-1}\times\\ \times\sum_{i=1}^{i=n}\delta_\varepsilon\left(\left\|{}_{(2)}\underline{a}-{}_{(2)}\underline{a}_i\right\|\right)\,\gamma_i\,\underline{\underline{\widehat{W}}}_{\mathrm{i}}^{\mathrm{T}}\,\left[{}_{(4)}\underline{a}_i-\underline{\breve{W}}_i\right]\end{aligned} \tag{57}$$

which allows to compute at each $_{(2)}\underline{a}$ the closure relation coefficients $\underline{\beta}_d$ and then from Eq. (51) $\underline{\beta}_u$ which defined completely the closure relation:

$$_{(4)}\underline{a} = =\underline{\underline{W}}(_{(2)}\underline{a})\underline{\beta}(_{(2)}\underline{a}) \tag{58}$$

Remark 3. If one consider a unit window function, i.e. $\delta_\varepsilon(d) = 1$, it results a global least squares approximation that implies that closure coefficient does not depend anymore on $_{(2)}\underline{a}$.

3. Numerical tests

3.1 *Simple shear flow*

We consider a 2D simple shear flow whose kinematics is defined by $\underline{v}^T = (\dot{\gamma} y,\ 0)$ being the shear rate $\dot{\gamma} = 1$. The fiber suspension is characterized by fibers whose shape factor leads to $k = 0.8$ and the diffusion coefficient was set to $D_r = 0.1$. The orientation distribution (assumed 2D) is discretized using the SUPG finite element method on the mesh associated with the conformation space that consists of $N_c = 200$ nodes uniformly distributed in $[0, 2\pi[$.

When the Fokker-Plank equation is integrated along a trajectory from the isotropic initial state until reaching the steady state characterized by a small enough variation between two consecutive time steps, that is:

$$\left\| \underline{\psi}(t_{n+1}) - \underline{\psi}(t_n) \right\| \le 10^{-6} \left\| \underline{\psi}(t_1) - \underline{\psi}(t_0) \right\|$$

and the Karhunen-Loève decomposition is applied to the snapshots selected during the orientation distribution evolution (around 20), the modes depicted in figure 1 are then obtained.

We can notice that the linear combination of only 5 orientation distributions (the ones depicted in figure 1) are enough to represent accurately the evolution of the orientation distribution along the considered streamline. It is also important to remark that these functions have not a full physical meaning, because, for

example, they take negative values. However their linear combination can reproduce perfectly the evolution of the distribution function coming from the resolution of the Fokker-Planck equation. However, in the procedure described in the previous section the second moment of those distributions (second order orientation tensor) is calculated, and due to the characteristics of those distributions the derived tensors have not a unit trace. Despite this fact one could continue to apply the procedure proposed in the previous section ignoring those physical or conceptual difficulties.

Other possibility to avoid these modes without a full physical meaning, consists of assuming that the orientation distribution can be written everywhere on the considered streamline as a linear combination of some orientation distributions (snapshots), for example, those were used for applying the Karhunen-Loève decomposition. In order to avoid the consideration of two distributions too close, one could start with the initial distribution, adding a new distribution to the reduced approximation basis only when it is far enough from all the functions defining the reduced approximation basis. The advantage of this approach is that all the modes used for approximating the orientation distribution evolutions are real physical distributions and consequently the associated second order orientation tensors are perfectly defined from all points of view. Figure 2 shows the different modes defined on the same streamline by using the just described strategy. We can notice the smoothness, periodicity, definite positive and normality of those distributions that define the reduced approximation basis which also contains 5 functions.

Finally, one could consider a last possibility related to the snapshot proper orthogonal decomposition. This technique is based on finding the significant modes from the application of the Karhunen-Loève decomposition, but assuming that those modes can be written as a linear combination of the N_{snap} snapshot that were used to define the decomposition. The main advantage of this strategy derives from the fact that it is easy to prove that theses modes result from the eigenproblem defined by

$$\left(\underline{\underline{Q}}^T \underline{\underline{Q}}\right) \underline{\Upsilon} = \lambda \underline{\Upsilon} \tag{59}$$

whose size is $N_{snap} \times N_{snap}$ instead of $N_c \times N_c$, and where only the eigenvectors related to large enough eigenvalues are retained, $\lambda_i > 10^{-8} \lambda_1$, λ_1 being the highest eigenvalue. From those eigenvectors the

reduced approximation modes are computed using the fact that those modes are linear combination of the snapshots, i.e.:

$$\underline{\phi}_i = \underline{\underline{Q}}\ \underline{\Upsilon}_i, \qquad \mathrm{i} \in \left[1, \cdots, n\right] \tag{60}$$

The most significant modes $\underline{\phi}_i$ related to the eigenvectors $\underline{\Upsilon}_i$ through $\underline{\phi}_i = \underline{\underline{Q}}\ \underline{\Upsilon}_i$ are depicted in figure 3.

In any case, these three numerical schemes offer three reduced approximation basis that can be used to define the natural closure according to the procedure defined in the previous section.

In order to compare these different strategies, we have computed the reference second order orientation tensor from the resolution of the Fokker-Planck equation, and then the different orientation tensors using the closures proposed in the previous section. The reference and approximated second order orientation tensors were compared at different times, for different values of the diffusion coefficients, using the following error measure:

$$E = \left\| \underline{\underline{a}}^{ref} - \underline{\underline{a}}^{aprox} \right\| \tag{61}$$

Table 1 groups the different computed errors at the end of the evolution process. We can notice that when the diffusion coefficient is small enough the standard natural closure relation works perfectly because we are close to the hypothesis under which it was derived. However, when the diffusion coefficient is increased, the solution accuracy is degraded. On the other hand, the adaptive natural closure that we have defined works perfectly for any diffusion coefficient, except for the too small values that induce numerical difficulties in the finite element discretization of the Fokker-Planck equation in the conformation space. We must mention that due to the fact that the Karhunen-Loève and the Snapshot Karhunen-Loève natural closures are built from modes (approximation functions) that have not a full physical meaning we have preferred using a global least square technique. Moreover, the global least squares fitting can be applied without a significant impact on the solution accuracy and with a considerable computing time reduction.

3.2 *Extensional flow*

We consider a 2D extensional flow whose kinematics is defined by $\underline{v}^T = (\dot{\varepsilon} x, \ -\dot{\varepsilon} y)$ being the elongation rate $\dot{\varepsilon} = 1$. The fiber suspension is characterized by fibers whose shape factor leads to $k = 0.8$. The orientation distribution (assumed 2D) is discretized using the SUPG finite element method on the mesh associated with the conformation space that consists of $N_c = 200$ nodes uniformly distributed in $[0, 2\pi[$.

Figures 4 and 5 depict the time evolution of the error defined in Eq. (61) for $D_r = 0.01$ and $D_r = 0.1$ respectively, where only the snapshot natural closure is compared with the standard natural one. We can notice the superior accuracy of the snapshot natural closure for both diffusion coefficients.

3.3 ***Driven cavity flow model: an example of complex flow***

In this section we consider the complex flow generated in a driven cavity $\Omega =]0,1[\times]0,1[$ that involves a short fiber suspension characterized by the same material parameters that in the previous tests. The velocity is prescribed on the domain boundary according to: $\underline{v}(x=0,y) = \underline{v}(x=1,y) = \underline{v}(x,y=0) = \underline{0}$ and $\underline{v}(x,y=1)^T = \left(16 v_{\max} x^2 (1-x)^2, 0\right)$. The velocity field is then solved by assuming a Newtonian behavior and by applying a standard mixed finite element formulation where the velocity and pressure approximations verify the LBB stability condition. The Fokker-Planck equation governing the evolution of the fiber orientation distribution function is then solved along some closed streamlines, where the periodicity condition of that distribution function was imposed as described in Ammar and Chinesta (2005). From the computed orientation distribution function, the characteristic modes are extracted by using the technique previously described based on the application of the Karhunen-Loève decomposition, allowing to fit the empirical natural closure introduced in section 2.3 using the snapshot natural closure strategy previously introduced. Now, the evolution equation associated with the second order orientation tensor is solved by assuming different closure relations: linear, quadratic, hybrid, natural and the empirical natural one.

If the Fokker-Planck equation is solved in the whole domain considering a fine enough mesh, the fiber distribution function can be computed everywhere without addressing any closure relation. Thus, the second order orientation tensor related to the just computed distribution function can be used as reference solution for comparison purposes.

The error between the computed second order orientation tensor and the reference solution coming from the solution of the Fokker-Planck equation is reported in Table 2.

From the previous results we can conclude that in the case of real complex flows it is difficult to conclude about the net superiority of a particular closure relation. In this kind of flows there are regions in which advection terms dominate the diffusion ones (as for example in the neighborhood of the upper wall in the driven cavity flow) whereas in others regions diffusion terms dominate the advection ones. The contrast between these two competitive behaviors increases as the diffusion coefficient decreases because for high enough diffusion coefficients the spatial gradients of the orientation field are quite reduced.

4. Conclusions

This work focused on the resolution of the Fokker-Planck equation that governs the evolution of the fiber orientation distribution. To reduce the computing time, that equation is solved along some flow trajectories in order to extract the significant information of the solution from the application of the Karhunen-Loève decomposition. This extraction has been made using three different strategies: (i) the standard Karhunen-Loève decomposition; (ii) the simple use of some snapshots of the orientation distribution evolution (linear independence is checked during the basis construction) and (iii) applying the snapshot-Karhunen-Loève decomposition that makes optimal the snapshot basis. From this reduced approximation bases we adjust a closure relation that becomes optimal for such flow, that allows solving the evolution of some orientation moments which require a less amount of computation. The accuracy of the proposed approach has been illustrated in some numerical examples concerning some simple flows, and seems to be an appealing strategy when the salient diffusion effects have an unfavourable effect on the natural closure approximation. Thus, a mixed strategy combining the natural closure in the regions where the orientation is dominated by

advection terms and the adjustable one when the diffusion effects becomes important could be nice candidate to be considered when fast and accurate solutions are desired.

REFERENCES

S.G. Advani, Ch.L.Tucker III. Closure approximations for three-dimensional structure tensors. J. Rheol., 34, 367-386, (1990).

A. Ammar, F. Chinesta. A particle strategy for solving the Fokker-Planck equation governing the fiber orientation distribution in steady recirculating flows involving short fiber suspensions. Lectures Notes on Computational Science and Engineering, Springer, 43, 1-16, (2005).

G.K Batchelor. Slender-body theory for particles of arbitrary cross-section in Stokes flow. J. Fluid Mech., 44, 419-440, (1970).

C. Chauviere, A. Lozinski. Simulation of dilute polymer solutions using a Fokker-Planck equation. Computers and Fluids., 33, 687-696 (2004).

F. Dupret, V. Verleye. Modelling the flow of fiber suspensions in narrows gaps. In Advances in the Flow and Rheology of Non-Newtonian Fluids. D.A. Siginer, D. De Kee and R.P. Chabra editors, Rheology Series, Elsevier, 1347-1398, (1999).

F.P. Folgar, Ch.L. Tucker III. Orientation behavior of fibers in concentrated suspensions. J. Reinf. Plast. Comp., 3, 98-119, (1984).

F. Gillet-Chaulet, O. Gagliardini, J. Meyssonnier, T. Zwinger, J. Ruokolainen. Flow-induced anisotropy in polar ice and related ice-sheet flow modelling. J. Non-Newtonian Fluid Mech., 134, 33-43, (2006).

G.L. Hand. A theory of anisotropic fluids. J. Fluid Mech., 13, 33-46, (1962)

E.J. Hinch, L.G. Leal. Constitutive equations in suspension mechanics. Part I. J. Fluid Mech., 71, 481-495, (1975).

E.J. Hinch, L.G. Leal. Constitutive equations in suspension mechanics. Part II. J. Fluid Mech., 76, 187-208, (1976).

M.A. Hulsen, A.P.G. van Heel, B.H.A.A. van den Brule. Simulation of viscoelastic flows using Brownian configuration fields. J. Non-Newtonian Fluid Mech., 70, 79-101, (1997).

G.B. Jeffrey. The motion of ellipsoidal particles immersed in viscous fluid. Proc. R. Soc. London, Ser. A 102, 161-179, (1922).

G.G. Lipscomb, M.M. Denn, D.H. Hur, D.V. Boger. The flow of fiber suspensions in complex geometries. J. Non-Newtonian Fluid Mech., 26, 297-325, (1988).

A. Lozinski, C. Chauviere. A fast solver for Fokker-Planck equation applied to viscoelastic flows calculations: 2D FENE model. J. Computational Physics, 189, 607-625, (2003).

H.C. Öttinger, M. Laso. Smart polymers in finite element calculation. Int Congr. on Rheology, Brussel, Belgium (1992).

M. Parsheh, M.L. Brown, C.K. Aidun, Investigation of closure approximations for fiber orientation distribution in contracting turbulent flow. J. Non-Newtonian Fluid Mech., 136, 38-49, (2006).

D. Ryckelynck, F. Chinesta, E. Cueto, A. Ammar. On the a priori model reduction: overview and recent developments. Archives of Computational Methods in Engineering, 13/1, 91-128, (2006).

Ch.L. Tucker III. Flow regimes for fiber suspensions in narrow gap. J. Non-Newtonian Fluid Mech., 39, 239-268, (1991).

Diffusion	Natural Closure	KL - Natural Closure	Snapshot Natural Closure	Snapshot-KL Natural Closure
0.1	0.0139	0.0095	0.0091	0.0355
0.01	0.0046	0.0196	0.0113	0.0471

Table 1. Error of the different closure approximations: standard natural closure (Dupret and Verleye, 1999) and the adaptive natural closure described in section 2 using the three different reduced approximation bases just defined: the first one using the modes coming from the direct application of the Karhunen-Loève decomposition, the second one using some appropriate snapshots and the last one based on the use of the snapshot Karhune-Loève decomposition.

Diffusion	Linear	Quadratic	Hybrid	Natural	Empirical Natural
1	0.0031	0.0704	0.0062	0.0019	0.0008
0.1	0.1992	0.1516	0.0800	0.0353	0.0289
0.01	1.1286	0.1452	0.1048	0.1216	0.1126

Table 2. Error of the different closure approximations: linear, quadratic, hybrid, standard natural closure (Dupret and Verleye, 1999) and the snapshot natural closure described in section 2.

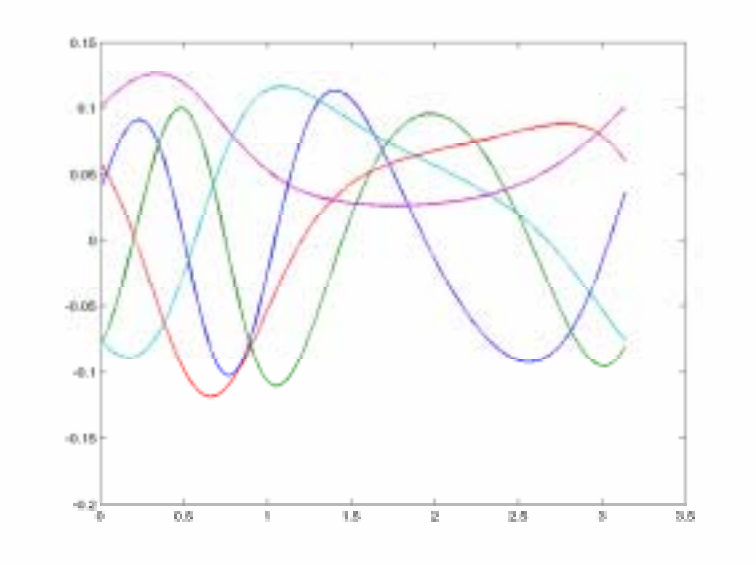

Figure 1. Significant modes related to the evolution of the orientation distribution function along a streamline computed from the Karhunen-Loève decomposition.

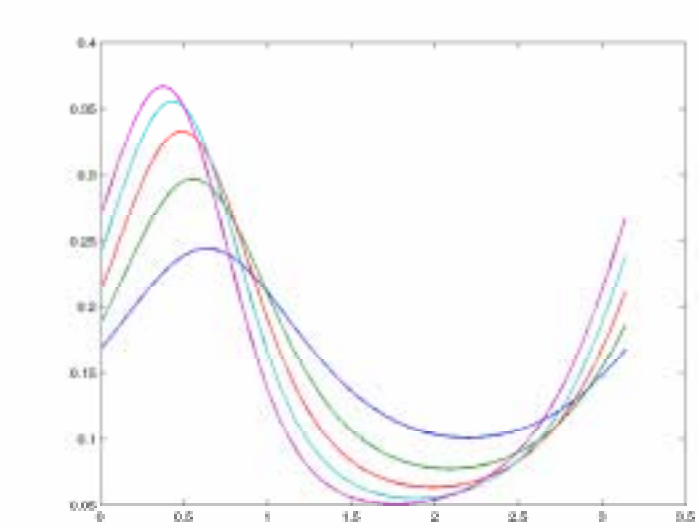

Figure 2. Reduced approximation modes related to the evolution of the orientation distribution function along a flow streamline.

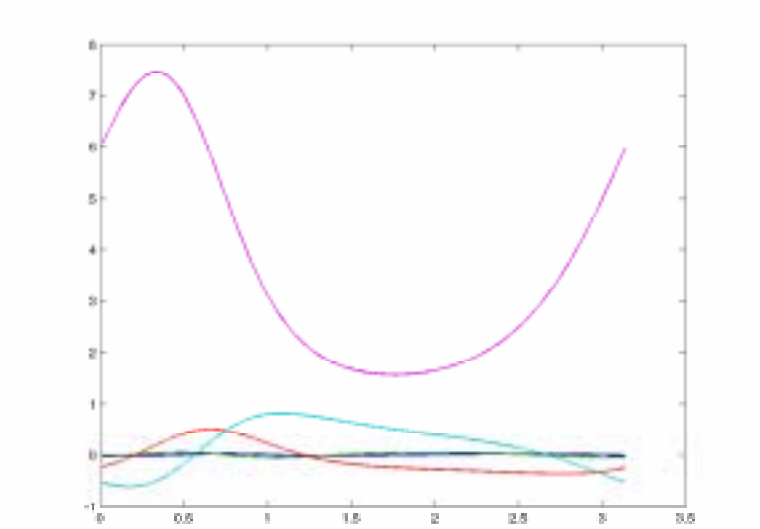

Figure 3. Significant modes related to the snapshot – Karhunen-Loève techniques.

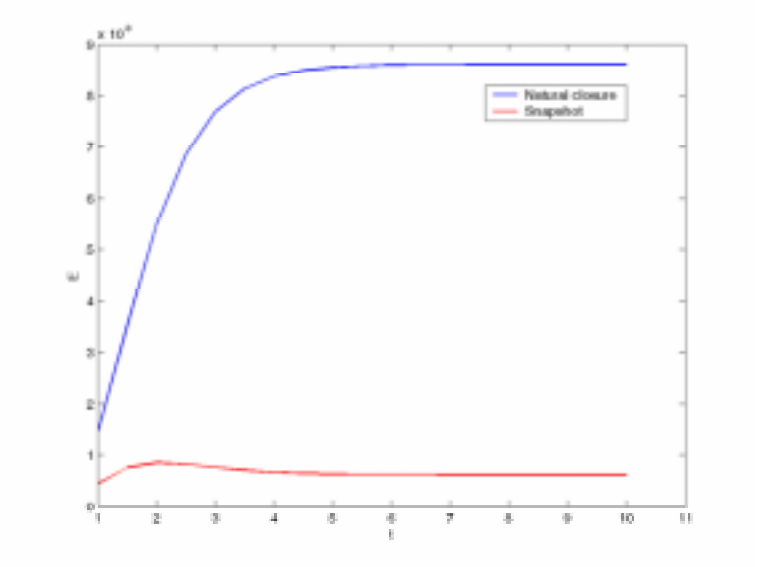

Figure 4. Error evolution in an elongational flow for $D_r = 0.01$

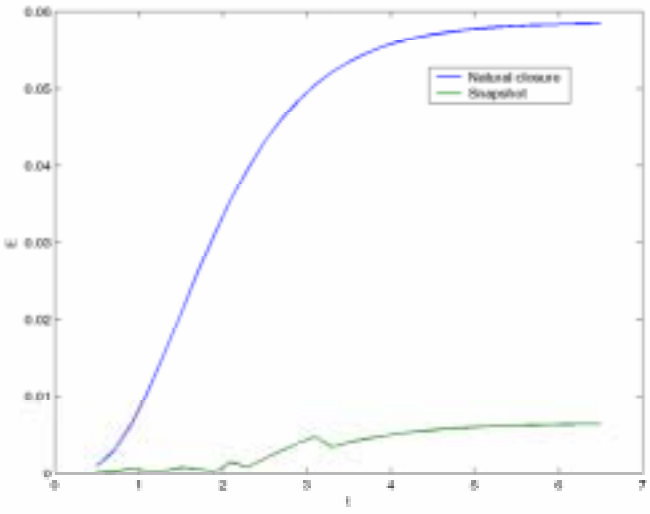

Figure 5. Error evolution in an elongational flow for $D_r = 0.1$